

Ligand-Controlled Chemoselective C(acyl)-O bond vs. C(aryl)-C bond Activation of Aromatic Esters in Nickel Catalyzed C(sp²)-C(sp³) Cross-Couplings

Adisak Chatupheeraphat, Hsuan-Hung Liao, Watchara Srimontree, Lin Guo, Yuri Minenkov, Albert Poater, Luigi Cavallo, and Magnus Rueping

J. Am. Chem. Soc., **Just Accepted Manuscript** • DOI: 10.1021/jacs.7b12865 • Publication Date (Web): 20 Feb 2018

Downloaded from <http://pubs.acs.org> on February 20, 2018

Just Accepted

“Just Accepted” manuscripts have been peer-reviewed and accepted for publication. They are posted online prior to technical editing, formatting for publication and author proofing. The American Chemical Society provides “Just Accepted” as a service to the research community to expedite the dissemination of scientific material as soon as possible after acceptance. “Just Accepted” manuscripts appear in full in PDF format accompanied by an HTML abstract. “Just Accepted” manuscripts have been fully peer reviewed, but should not be considered the official version of record. They are citable by the Digital Object Identifier (DOI®). “Just Accepted” is an optional service offered to authors. Therefore, the “Just Accepted” Web site may not include all articles that will be published in the journal. After a manuscript is technically edited and formatted, it will be removed from the “Just Accepted” Web site and published as an ASAP article. Note that technical editing may introduce minor changes to the manuscript text and/or graphics which could affect content, and all legal disclaimers and ethical guidelines that apply to the journal pertain. ACS cannot be held responsible for errors or consequences arising from the use of information contained in these “Just Accepted” manuscripts.



Ligand-Controlled Chemoselective C(acyl)-O bond vs. C(aryl)-C bond Activation of Aromatic Esters in Nickel Catalyzed C(sp²)-C(sp³) Cross-Couplings

Adisak Chatupheeraphat,^{§,†} Hsuan-Hung Liao,^{§,†} Watchara Srimontree,[†] Lin Guo,[†] Yury Minenkov,[‡] Albert Poater,^{‡,#} Luigi Cavallo,[‡] and Magnus Rueping^{†,‡}

[†]Institute of Organic Chemistry, RWTH Aachen University, Landoltweg 1, 52074 Aachen, Germany

[‡]King Abdullah University of Science and Technology (KAUST), KAUST Catalysis Center (KCC), Thuwal 23955-6900, Saudi Arabia

[#]Institut de Química Computacional i Catàlisi and Departament de Química, Universitat de Girona, Campus Montilivi, 17003 Girona, Catalonia, Spain

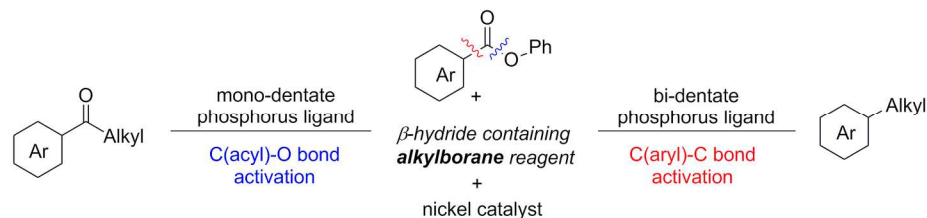
KEYWORDS. Nickel catalysis, C-C bond formation, cross coupling

ABSTRACT: A ligand-controlled and site-selective nickel catalyzed Suzuki-Miyaura cross-coupling reaction with aromatic esters and alkyl organoboron reagents as coupling partners was developed. This methodology provides a facile route for C(sp²)-C(sp³) bond formation in a straightforward fashion by successful suppression of the undesired β-hydride elimination process. By simply switching the phosphorus ligand, the ester substrates are converted into the alkylated arenes and ketone products respectively. The utility of this newly developed protocol was demonstrated by its wide substrate scope, broad functional group tolerance and application in the synthesis of key intermediates for the synthesis of bioactive compounds. DFT studies on the oxidative addition step helped rationalizing this intriguing reaction chemoselectivity: whereas nickel complexes with bidentate ligands favor the C(aryl)-C bond cleavage in the oxidative addition step leading to the alkylated product via a decarbonylative process, nickel complexes with mono-dentate phosphorus ligands favor activation of the C(acyl)-O bond, which later generates the ketone product.

■ INTRODUCTION

The discovery and development of transition metal catalyzed cross-coupling reactions is one of the most successful chapters in modern organic chemistry. Among the disclosed transformations, the Suzuki-Miyaura cross-coupling reaction has emerged as a powerful tool¹ to forge linkages between carbon atoms. To date most coupling reactions show superior ability for the synthesis of non-symmetric biaryls via C(sp²)-C(sp²) cross-coupling,² while the development of C(sp²)-C(sp³) bond formations is still more difficult to accomplish,^{3,4} and suffers from several undesired reaction pathways. For example, β-hydride elimination and protodeboration⁵ plague the transfer of the alkyl residue from the organometallic reagent to the organic framework, which makes the development of C(sp²)-C(sp³) couplings a tedious exercise.

Conventionally, halocarbon electrophiles are the most applied coupling partners in Suzuki-Miyaura reactions. However, the corrosive halide-containing waste production does not meet the modern synthetic chemistry expectations with the growing interest in environmentally friendly protocol development nowadays. In this context, aroyl compounds, due to their ubiquitous nature, have received considerable attention to further complement organic halides as coupling partners in the realm of transition metal catalyzed reactions.⁶⁻⁸ Early examples of using aroyl electrophiles in a decarbonylative manner focused on “active” species, such as acid chlorides,⁶ anhydrides,⁷ or twisted amides.⁸ The concept of using naturally abundant and “non-activated” esters in decarbonylative cross-couplings is still in its infancy,⁹ perhaps due to the difficulty in finding a suitable catalyst for the activation of inert bonds.



Scheme 1. Ligand-Controlled Ni-Catalyzed Suzuki-Miyaura cross-coupling reaction: C(acyl)-O bond vs. C(aryl)-C bond activation.

Palladium catalysis has historically dominated the field of C-halogen bond activation; however, first row transition metals, such as nickel, were found to be more effective alternatives to harness less reactive electrophiles.¹⁰ For example, the electron-rich nature renders nickel to be more reactive toward strong bond activation, such as C-O bonds, in the oxidative addition step. Furthermore, β -hydride elimination is a minor issue with nickel compared with palladium due to the high energy barrier of nickel-carbon bond rotation.¹¹

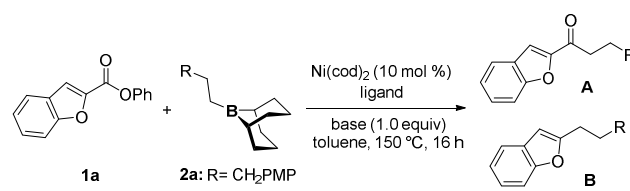
Hence, the development of a nickel catalyzed Suzuki-Miyaura decarbonylative cross-coupling variant¹² with alkylboron compounds and phenyl esters as cross-coupling partners would enable an important advancement in the formation of C(aryl)-C(alkyl) bonds (Scheme 1). On the other hand, alkyl ketones are important motifs in many natural products and pharmaceutical compounds. Besides, their propensity to undergo further functional group interconversion makes them valuable synthetic intermediates. Commonly used transition metal catalyzed methods to synthesize ketones include: 1) transition-metal-catalyzed carbonylation of organic halides (RX) with CO; 2) nucleophilic addition of organometallics to carboxylic acid derivatives. However, the manipulation of toxic carbon monoxide under high pressure conditions limits the carbonylation strategy and the overaddition of hard organometallic reagents to carboxylic acid derivatives often results in the formation of undesired tertiary alcohols instead of ketones.¹³ Therefore, a user-friendly synthetic operation which can produce solely ketone products is highly desired. Transition-metal-catalyzed Suzuki-Miyaura cross-coupling is an ideal platform for such transformations¹⁴ and progress in acylation reactions was accomplished by using reactive acylating reagents such as acid chlorides,¹⁵ acid anhydrides¹⁶ and thioesters.¹⁷ In addition, amide C-N bond cleavage became a recent topic;¹⁸ however, the reaction outcome is highly dependent on the protecting group on the amide moiety. In contrast, the activation of the acyl C-O bond of esters remains elusive. Inspired by Yamamoto's pioneering work in 1980,¹⁹ who reported the C-O bond cleavage of esters with stoichiometric amounts of Ni, Chatani's activation of pyridyl esters and their reaction with organoboron nucleophiles,²⁰ as well as Yamaguchi and Itami's report on the Ni catalyzed decarbonylative coupling of azoles with aromatic esters^{9f} we questioned whether a Suzuki-Miyaura coupling system could be extended to simple and unactivated phenyl esters, suppressing the loss of carbonyl moiety (CO) for the ketone formation.

The development of readily tunable and chemoselective transformations in the presence of multiple possible reactive sites is a challenge in modern organic synthesis. Transition metal catalyzed reactions are effective in addressing this problem by changes in the coordination geometry of the catalytic center using diverse ligand effects. Herein, we describe a ligand switchable Suzuki-Miyaura cross-coupling variant with ester and alkyl organoboron components as coupling partners. This newly developed methodology provides an unconventional route for C(sp²)-C(sp³) bond formation in a straightforward fashion, which successfully suppresses the undesired β -hydride elimination. Furthermore, the judicious choice of different phosphorus ligands delivers the decarbonylative and ketone products respectively (Scheme 1).²¹

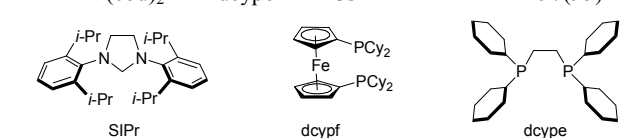
RESULTS AND DISCUSSION

Guided by the theory mentioned above, survey coupling experiments with phenyl benzofuran-2-carboxylate **1a** and B-alkyl-9-BBN **2a** under Ni(cod)₂ [cod = 1,5-cyclooctadiene] catalysis were carried out and the results are summarized in Table 1. Preliminary experiments were conducted with a series of trialkyl-monodentate phosphine ligands, including P^{*n*}Bu₃ and PCy₃ which resulted in a mixture of ketone **A** and decarbonylative product **B** (Table 1, entries 1-2). Carbene ligands such as 1,3-bis(2,6-diisopropylphenyl)imidazolidin-2-ylidene (SIPr) did not provide any trace of product (Table 1, entry 3). Further evaluation of a range of bidentate phosphine complexes revealed the complete suppression of undesired ketone by-product formation (Table 1, entries 4-5). The most competent ligand was identified as dcype [1,2-bis(dicyclohexylphosphino) ethane] providing the product in 75% yield (Table 1, entry 5). Regarding the effect of different bases (Table 1, entries 5-7), the best result in terms of reactivity was obtained with CsF as base (Table 1, entry 5). The base plays a crucial role in the transmetalation step, where a higher free bond enthalpy of the newly formed boron-base bond could provide a better driving force for the transmetalation process. Owing to the fact that boron-fluorine bonds are the strongest single bonds (B-F bond is 146 kcal/mol),²² the fluoride salt shows superior ability among the others.

Table 1. Optimization of the nickel catalyzed decarbonylative C_{sp2}-C_{sp3} coupling^a



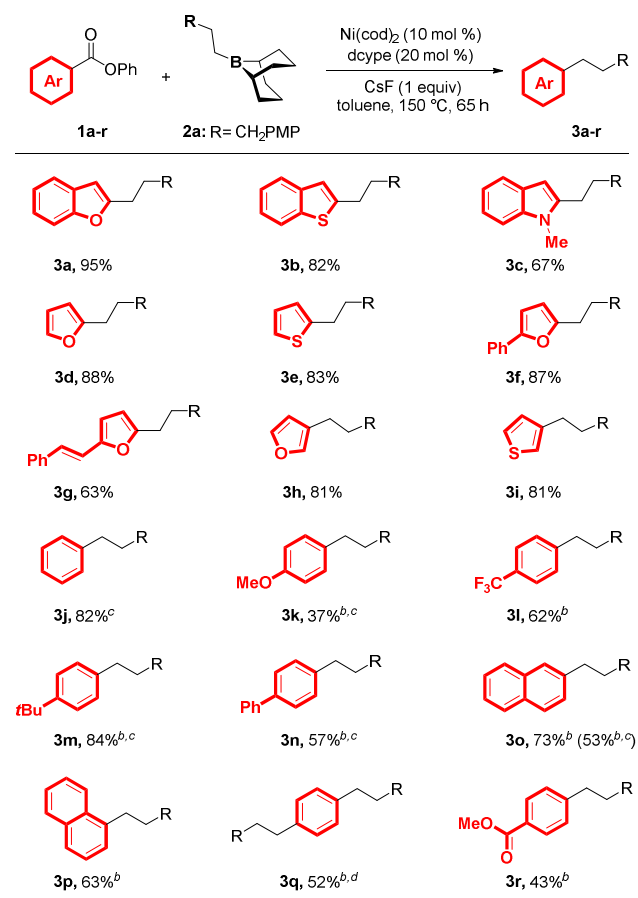
Entry	Ni cat.	Ligand	Base (1 equiv)	Yield ^b (%)	
				A	B
1	Ni(cod) ₂	P ^{<i>n</i>} Bu ₃	CsF	5	14
2	Ni(cod) ₂	PCy ₃	CsF	10	-
3	Ni(cod) ₂	SIPr	CsF	-	-
4	Ni(cod) ₂	dcypf	CsF	-	40
5	Ni(cod) ₂	dcype	CsF	-	75
6	Ni(cod) ₂	dcype	Cs ₂ CO ₃	-	6
7	Ni(cod) ₂	dcype	K ₃ PO ₄	-	39
8	Ni(cod) ₂	dcype	-	-	23
9 ^c	Ni(cod) ₂	dcype	CsF	-	41
10 ^d	Ni(cod) ₂	dcype	CsF	-	66
11	NiCl ₂ /Zn	dcype	CsF	-	20
12	-	dcype	CsF	-	-
13 ^e	Ni(cod) ₂	dcype	CsF	-	98(95) ^f
14 ^{d,e}	Ni(cod) ₂	dcype	CsF	-	97(95) ^f



^aReaction conditions: **1a** (0.2 mmol), **2a** (0.4 mmol), Ni(cod)₂ (10 mol %), ligand (40 mol %), base (1.0 equiv), toluene (1 ml), 150 °C, 16 h. ^bNMR yield, 1,3,5-(OMe)₃C₆H₃ as internal standard. ^cReaction in *i*-Pr₂O. ^ddcype (20 mol %). ^eReaction performed for 72 h. ^fYield of isolated product.

Interestingly, a base-free reaction still successfully delivered the desired product, albeit with a much lower yield (Table 1, 23% vs. 75% yield, entry 8 vs. 5). Further optimization focused on solvent screening; switching the solvent from toluene to diisopropyl ether, however, afforded a lower yield (Table 1, entry 9). In situ generation of the Ni (0) catalyst from NiCl₂ and zinc dust was evaluated; however, a significantly decreased reactivity was observed (Table 1, 20% vs. 75% yield, entry 11 vs. 5). Control reactions showed that no product is obtained in the absence of the nickel catalyst (Table 1, entry 12). Notably, extending the reaction time afforded the product in better yield (Table 1, entry 5 vs. 13 and entry 10 vs. 14). To further demonstrate the generality of this novel protocol, we evaluated the scope of the nickel catalyzed Suzuki-Miyaura cross-coupling reaction between esters and *B*-alkyl-9-BBNs. As revealed in Table 2, a variety of ester substrates with different electronic properties and substitution patterns provided the corresponding decarbonylative products **3** with excellent reactivity.

Table 2. Ester scope in the nickel catalyzed decarbonylative aryl-alkyl cross-coupling^a

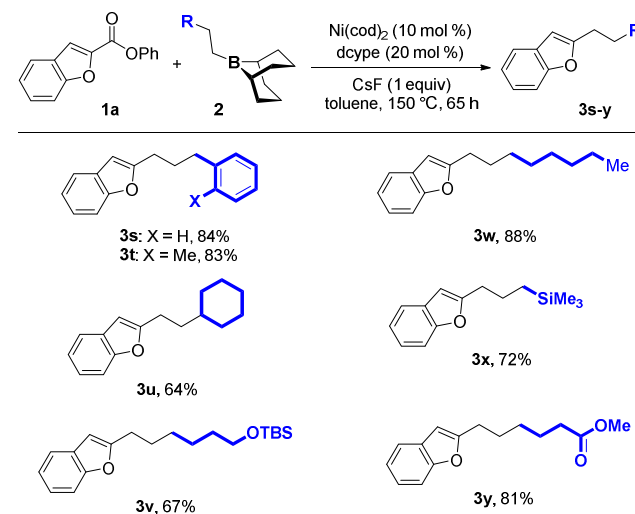


^aReaction conditions: **1** (0.2 mmol), **2a** (0.4 mmol), Ni(cod)₂ (10 mol %), dcype (20 mol %), CsF (1.0 equiv) in toluene (0.2 M) at

150 °C for 65 h, yield for isolated products. ^bdcype (40 mol %) was used. ^cCs₂CO₃ (2 equiv). ^dReaction was stirred for 5 days.

Initially, esters incorporating a series of different heterocyclic patterns, including benzofuran, benzothiophen and indole, were tested and the corresponding products **3a-c** were isolated with high yields (95, 82, and 67% yield respectively). Switching to structurally simpler furan and thiophene based esters still provided the products **3d-i** with pleasing results. Further efforts focused on non-heteroatom containing aromatic moieties on the ester group. Substrates with non-substituted (**1j**), electron-rich (**1k**, **1m**) and -deficient (**1l**) phenyl esters were tested and participated ideally in this process, furnishing the corresponding adducts **3j-m** in moderate to good yields. In addition, substrates with π -extended aromatic rings, including biphenyl, 2-naphthyl and 1-naphthyl esters (**1n-p**) were also studied and provided satisfying results. Lastly, the chemoselectivity between different esters was also investigated. Notably, only the phenyl-containing ester moieties had been replaced and delivered the corresponding substituted product **3r**.

Table 3. Scope of organoborane in the nickel catalyzed decarbonylative aryl-alkyl cross-coupling^a



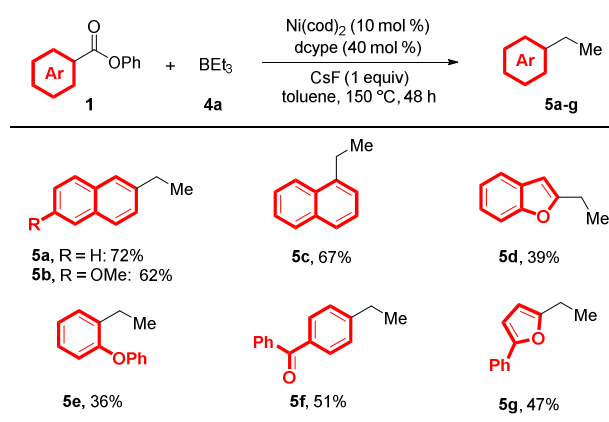
^aReaction conditions: **1a** (0.2 mmol), **2** (0.4 mmol), Ni(cod)₂ (10 mol %), dcype (20 mol %), CsF (1.0 equiv) in toluene (0.2 M) at 150 °C for 65 h, yield for isolated products.

After testing the tolerance with different ester precursors, our efforts focused on applying various *B*-alkyl-9-BBNs **2** in this newly developed Suzuki-Miyaura reaction. Different substitution patterns and electronic properties on the *B*-alkyl-9-BBNs were evaluated to establish the reaction scope. As shown in Table 3, all alkylborane reagents were well tolerated and the decarbonylative products **3s-y** were isolated in good yields. Furthermore, the silyl and ester group containing alkylborane nucleophiles were also suitable for the cross-coupling protocol, which features the possibility for further functional group interconversion.

In addition to the *in situ* prepared *B*-alkyl-9-BBN nucleophiles, commercial available triethylborane (BET₃) has also proved itself as an ideal alkylborane reagent for this demanding transformation. A series of different esters with aromatic and heteroatom containing aromatic moieties were employed

in this reaction under the optimized conditions and the corresponding products **5a-g** were obtained in good yields (Table 4).

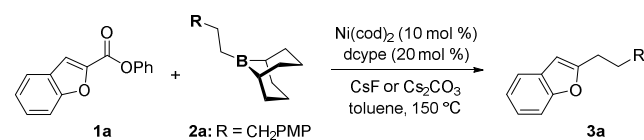
Table 4. Scope of the nickel catalyzed decarbonylative aryl-alkyl cross-coupling: Triethylborane as organoborane reagent^a



^aReaction conditions: **1** (0.2 mmol), **4a** (0.4 mmol), Ni(cod)₂ (10 mol %), dcype (40 mol %), CsF (1.0 equiv) in toluene (0.3 M) at 150 °C for 48 h, yield for isolated products.

Microwave irradiation has become a popular technique in modern transition metal catalysis, not only because it provides a highly efficient energy source, but also prevents the decomposition of sensitive catalysts.²³ Therefore, we became interested in a microwave-assisted procedure for our newly developed nickel catalyzed decarbonylative C^{sp2}-C^{sp3} coupling. When compared to the batch reaction, an enormous process acceleration was observed (Table 5, entry 1 vs entry 2).

Table 5 Nickel catalyzed decarbonylative C_{sp2}-C_{sp3} couplings: MW vs. Batch^a



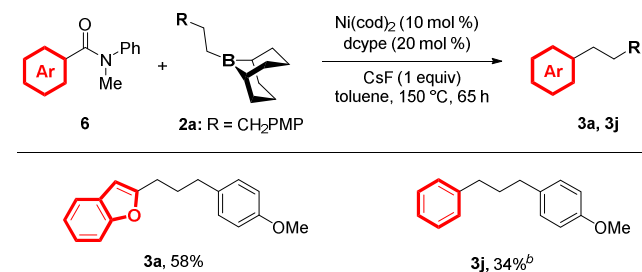
Entry	Conditions	Time (h)	Yield ^b (%)
1	MW	5	82
2	Batch	5	39
3 ^c	MW	5	64

^aReaction conditions: **1a** (0.2 mmol), **2a** (0.4 mmol), Ni(cod)₂ (10 mol %), dcype (20 mol %), CsF (1.0 equiv), toluene (1 ml). ^bNMR yield, 1,3,5-(OMe)₃C₆H₃ as internal standard. ^cWith Cs₂CO₃ (2 equiv) as base.

Inspired by the successful development of nickel catalyzed decarbonylative reactions with amide substrates reported independently by Szostak and Shi last year,²⁴ we also applied our optimal reaction conditions to amides as substrates in this new Suzuki-Miyaura cross-coupling reaction (Table 6). Within this area, we were interested to forge linkages between C(sp²) and C(sp³) atoms from un-activated amides which is challenging and difficult to achieve. To our delight, the benzofuryl- and phenyl-based amides were successfully transformed into the

desired alkylated products **3a**, **3j** with 58% and 34% yields respectively.

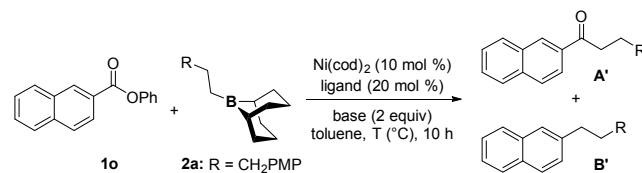
Table 6. Scope of the nickel catalyzed decarbonylative aryl-alkyl cross-coupling with amides^a



^aReaction conditions: **6** (0.2 mmol), **2a** (0.4 mmol), Ni(cod)₂ (10 mol %), dcype (20 mol %), CsF (1.0 equiv) in toluene (0.2 M) at 150 °C for 65 h, NMR yield, 1,3,5-(OMe)₃C₆H₃ as internal standard. ^b160 °C, 120 h.

We next turned our attention to the development of a general protocol for the ketone formation, which was isolated as a side product in our initial studies. The ketone product can be obtained from transmetalation with the B-alkyl-9-BBN without CO extrusion. Based on this observation, we hypothesized that the ketone might indeed become the sole product by varying the reaction parameters. Our initial efforts focused on screening various ligands.

Table 7. Optimization of the nickel catalyzed Suzuki-Miyaura cross-coupling reaction for ketone formation^a



Entry	Ligand	Base (2 equiv)	T (°C)	Yield ^b (%)	
				A'	B'
1	SIPr	Cs ₂ CO ₃	110	-	-
2	dcype	Cs ₂ CO ₃	110	-	-
3	dcype	Cs ₂ CO ₃	150	-	32
4 ^c	dcype	Cs ₂ CO ₃	150	-	42
5 ^{c,d}	dcype	Cs ₂ CO ₃	150	-	53
6 ^{d,e}	dcype	Cs ₂ CO ₃	150	-	61
7	PPh ₃	Cs ₂ CO ₃	110	12	-
8	PCy ₃	Cs ₂ CO ₃	110	82	-
9	P ⁿ Bu ₃	Cs ₂ CO ₃	110	90	-
10	P ⁿ Bu ₃	K ₃ PO ₄	110	50	-
11	P ⁿ Bu ₃	K ₂ CO ₃	110	40	-
12	P ⁿ Bu ₃	Na ₂ CO ₃	110	81	-
13 ^f	P ⁿ Bu ₃	Cs ₂ CO ₃	110	62	-
14	P ⁿ Bu ₃	Cs ₂ CO ₃	80	90	-
15	P ⁿ Bu ₃	Cs ₂ CO ₃	40	75	-
16 ^g	P ⁿ Bu ₃	Cs ₂ CO ₃	80	-	-
17	-	Cs ₂ CO ₃	80	-	-
18	P ⁿ Bu ₃	-	80	-	-

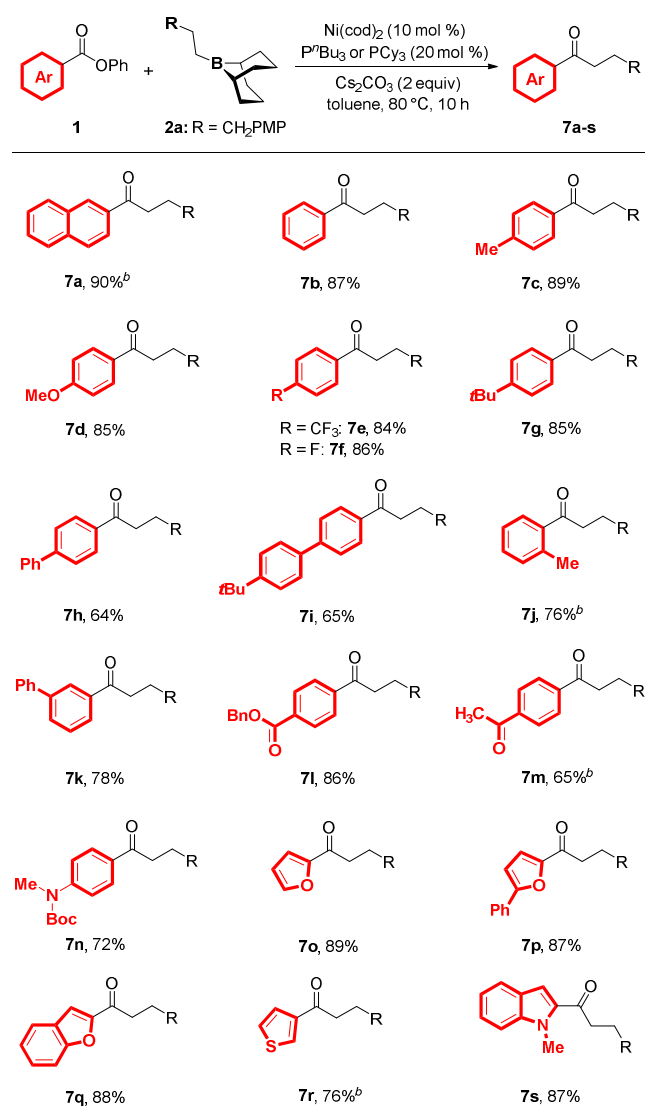
^aReaction conditions: **1o** (0.2 mmol), **2a** (0.4 mmol), Ni(cod)₂ (10 mol %), ligand (20 mol %), base (2 equiv), toluene (1 ml). ^bYield after purification. ^c65 h. ^ddcype (40 mol %). ^eReaction in MW for 5 h. ^fReaction in *i*-Pr₂O. ^gWithout Ni(cod)₂.

However, the carbene ligand, 1,3-bis(2,6-diisopropylphenyl)imidazolidin-2-ylidene (SIPr), and the bidentate phosphine ligand, 1,2-bis(dicyclohexyl-phosphino)ethane (dcype), did not provide the desired ketone product (Table 7, entries 1 and 2). In contrast, the corresponding decarbonylative product **B'** was obtained when the temperature of the reaction was raised to 150 °C and when the reaction was performed under microwave irradiation (Table 7, entries 3-6). Switching to monodentate phosphine ligands, including PPh₃, PCy₃ and P^{*n*}Bu₃, provided a significant improvement with regard to the reactivity and the desired ketone **A'** was isolated as the only product with 12%, 82% and 90% yield respectively (Table 7, entries 7-9), which indicates that the nature of the ligand has a dramatic effect on the reaction outcome. Continuing with the most promising ligand, P^{*n*}Bu₃, various bases were evaluated next. However, changing the base from cesium carbonate to other bases had a deleterious effect on the yield (Table 7, entries 10-12). Use of diisopropyl ether as solvent, provided a decrease in the reaction yield (Table 7, entry 13). Further optimization focused on the reaction temperature; lowering the reaction temperature to 80 °C was not detrimental for the ketone formation (Table 7, entry 14). Decreasing the reaction temperature further to 40 °C resulted in a lower yield (Table 7, entry 15). Lastly, a series of control experiments indicated that the presence of nickel catalyst, phosphorus ligand and base are crucial for the reaction (Table 7, entries 16-18).

Having established an optimal reaction protocol, an investigation of the substrate scope for the ketone formation was carried out. The results summarized in Table 8 show that a wide range of ester substrates are well tolerated in this C(acyl)-O bond activation protocol to afford the desired ketones **7a-s** with excellent reactivity.

Compared to the naphthyl substituted ketone **7a** (94%), the phenyl substituted ketone **7b** was also obtained with high yield (87%). This result indicated that reactive fused aromatic rings containing substrates are not necessary in this methodology. Therefore, we decided to examine the scope tolerance with simple phenyl substituted esters. Next, various phenyl-based esters bearing substituents with different electronic and steric properties in the *para* position were tested and the adducts **7c-i** were isolated in good to excellent yields (64-89%). Furthermore, phenyl-based esters with substitution on either *ortho* or *meta* positions also reacted nicely to furnish the desired ketone products **7j-k** with good yields (76-78%). In addition, the benzyl-based ester, methyl ketone and amine substitutions remained intact (**7l-n**). These versatile products show potential for further diversification via additional chemical transformations. Lastly, we also have evaluated substrates with heterocyclic moieties, including furan, benzofuran, thiophene and indole, which also gave the desired products with pleasing results (**7o-s**). The next aim was the application of this newly developed strategy to a variety of alkylborane reagents. In order to demonstrate the superiority of our protocol with respect to substrate scope tolerance, both the phenyl- and naphthyl-based esters were examined simultaneously.

Table 8. Ester scope for the nickel catalyzed cross-coupling reaction for ketone formation^a

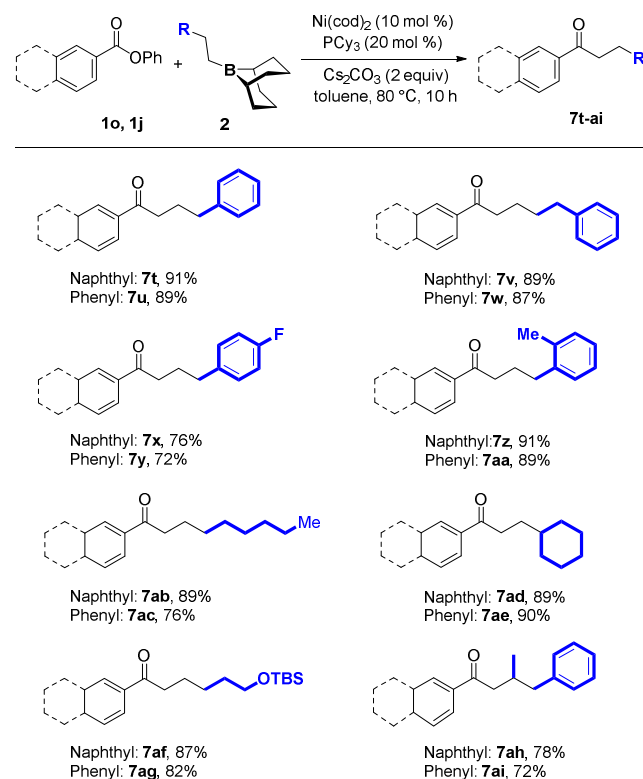


^aReaction conditions: **1** (0.2 mmol), **2a** (0.4 mmol), Ni(cod)₂ (10 mol %), PCy₃ (20 mol %), Cs₂CO₃ (2.0 equiv) in toluene (0.2 M) at 80 °C for 10 h, yield for isolated products. ^bP^{*n*}Bu₃ was used as ligand instead of PCy₃.

Firstly, various phenyl-based B-alkyl-9-BBNs **2** bearing substituents with different electronic properties in either *ortho* or *para* position were tested. Excellent results were achieved and adducts **7t-aa** were isolated in good to high yields (72-91%). Subsequently, aliphatic-based alkylborane reagents were applied, which also reacted nicely to furnish the corresponding ketones **7ab-ae** with high yields (76-90%). Furthermore, we also applied the silyl protected ether containing alkylborane reagent in the reaction system, which delivered the desired products **7af**, **7ag** with acceptable results (82-87% yield). Lastly, a chiral carbon containing reagent was found also suitable for the cross-coupling protocol. Subsequently, commercial available tri-alkyl boranes were subjected to the nick-

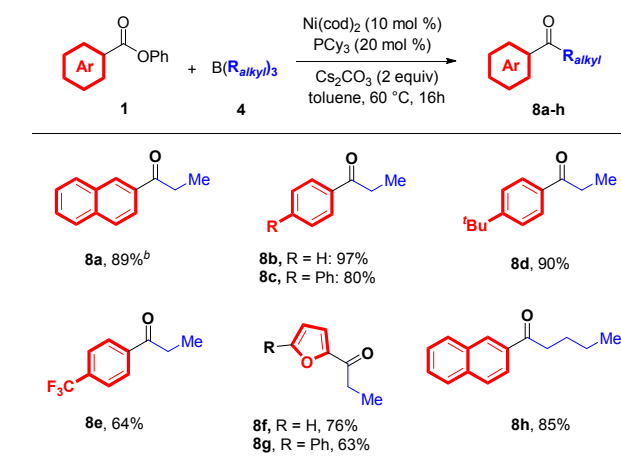
el-catalyzed reaction and coupled with a series of esters bearing different electronic properties (Table 10). To our delight, all applied substrates were successfully converted into the corresponding ketone products with good to excellent yields.

Table 9. Organoborane scope of the nickel catalyzed cross-coupling reaction for ketone formation^a



^aReaction conditions: **1o** or **1j** (0.2 mmol), **2** (0.4 mmol), Ni(cod)₂ (10 mol %), PCy₃ (20 mol %), Cs₂CO₃ (2.0 equiv) in toluene (0.2 M) at 150 °C for 10 h, yield for isolated products.

Table 10. Scope of the nickel catalyzed cross-coupling reaction for ketone formation: Trialkylborane as organoborane reagents^a



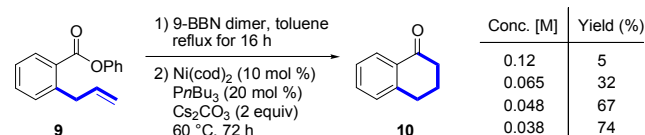
^aReaction conditions: **1** (0.2 mmol), **4a,b** (0.4 mmol), Ni(cod)₂ (10 mol %), PCy₃ (40 mol %), Cs₂CO₃ (2.0 equiv) in toluene (0.3 M) at 60 °C for 16 h, yield for isolated products. ^bReaction at 40 °C.

To show the synthetic applicability of our newly developed method, an intramolecular version of the nickel catalyzed Suzuki-Miyaura reaction was investigated. Conventionally, transition metal catalyzed intramolecular reactions sometimes suffer from undesired problems, e.g. self-dimerization. However, after reaction examination we were able to overcome the obstacle of undesired side product formation and to obtain the desired product **10** in good yield (Table 11).

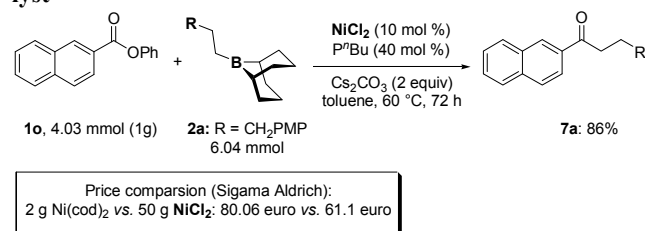
In a scale-up process, a gram scale reaction was carried out in order to demonstrate the scalability of our newly developed method. Importantly, the cheap and air stable NiCl₂ was found to be able to provide the ketone **7a** in high yield (86%),²⁵ which offers a great opportunity for further application in industry (Scheme 2).

The power of this methodology is exemplified through its application to the synthesis of bioactive reagents (Scheme 3). For examples, ester **1o** could be coupled with piperidine-derived organoborane reagent **11** under our optimal nickel catalyzed reaction conditions, which successfully provided ketone **12a** in 87% yield. Ketone **12a** is an intermediate for the synthesis of **13a**, a potent antagonist of α_vβ₃/α_vβ₅ integrins²⁶ and our cross-coupling strategy provides an alternative route for its synthesis. Compound **13b** which showed high affinity for selective serotonin reuptake inhibitors (SSRIs),²⁷ is expecting to produce a new generation of antidepressants with faster onset of action and greater efficiency and safety than the current marketed reagents. Therefore, we also applied our newly developed strategy to the synthesis of its ketone precursor **12b**, which was isolated in 82% yield.

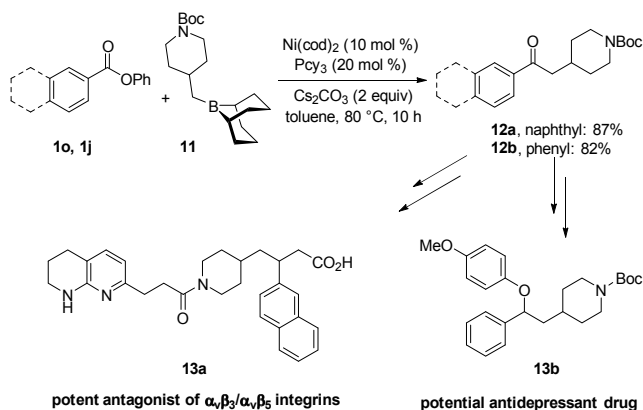
Table 11. Nickel catalyzed intramolecular Suzuki-Miyaura cross-coupling reaction



Scheme 2. Gram scale coupling: NiCl₂ as economical catalyst



Scheme 3. The developed alkylation method enables the facile synthesis of bioactive compounds



13
14 With this experimental background in mind²⁸ we performed
15 DFT calculations²⁹ to rationalize the selective activation of the
16 C(acyl)-O bond with mono-dentate phosphorus ligands versus the
17 selective activation of the C(aryl)-C bond with bi-dentate
18 phosphorus ligands.³⁰

19 As model system we investigated the reactivity of **1o** with
20 Ni(P^{*n*}Bu₃)₂ and Ni(dcype).

21 Focusing on Ni(P^{*n*}Bu₃)₂, the reaction starts with coordination
22 of the aryl ester **1o** to the Ni center to form complex **IN0** (Figure
23 1a). Oxidative addition of the C(acyl)-O bond to the metal
24 via transition state **TS1** requires an activation free energy of
25 22.7 kcal/mol to generate the acyl-Ni intermediate **IN1**. The
26 overall step is endergonic by 10.7 kcal/mol. The competitive
27 oxidative addition of the C(aryl)-C bond via transition state
28 **TS2**, generating intermediate **IN2**, has an activation barrier of
29 26.5 kcal/mol and it is endergonic by 11.1 kcal/mol. Thus,
30 with Ni(P^{*n*}Bu₃)₂ C(acyl)-O activation is favored over C(aryl)-
31 C bond activation by 3.8 kcal/mol (22.7 vs. 26.5 kcal/mol).
32 Oxidative addition at the O-C(phenyl) bond, via transition
33 state **TS3**, has an activation energy of 31.9 kcal/mol, excluding
34 this route.

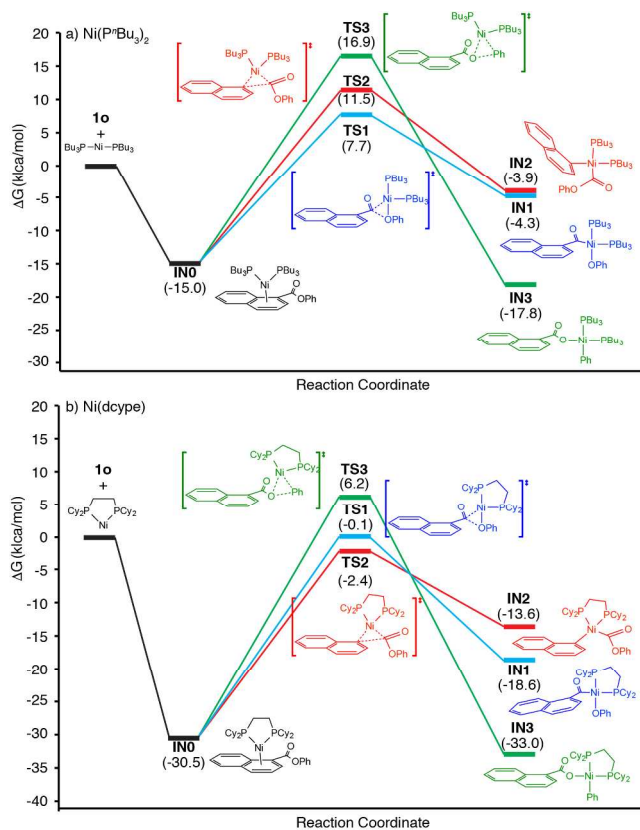


Figure 1. DFT-computed Gibbs free energy profile (in kcal/mol) for the oxidative addition of **1o** to: (a) Ni(P^{*n*}Bu₃)₂ and (b) Ni(dcype). Blue pathway: C(acyl)-O bond activation. Red pathway: C(aryl)-C bond activation. Green pathway: O-C(phenyl) bond activation.

Moving to Ni(dcype), coordination of **1o** to the Ni center to form complex **IN0** is exergonic by 30.5 kcal/mol (Figure 1b). Oxidative addition of the C(acyl)-O bond to the metal via transition state **TS1** requires an activation free energy of 30.4 kcal/mol to generate the acyl-Ni intermediate **IN1**, the overall step being endergonic by 11.9 kcal/mol. The competitive oxidative addition of the C(aryl)-C bond via transition state **TS2**, generating intermediate **IN2**, has an activation barrier of 28.1 kcal/mol and it is endergonic by 16.9 kcal/mol. Thus, Ni(dcype) activation of the C(aryl)-O bond is favored over activation of the C(acyl)-C bond by 2.3 kcal/mol (28.1 vs. 30.4 kcal/mol). Again oxidative addition of the O-C(phenyl) bond, via transition state **TS3** and an activation energy of 36.7 kcal/mol is at clearly higher energy, and thus it can be ruled out.

Having validated the computational protocol to reproduce the experimental selectivities, we moved to rationalize the origin of the different behavior. Comparison of the free energy profiles reported in Figures 1a and 1b indicates that the Ni(dcype) complex coordinates the substrate 15.5 kcal/mol stronger than the Ni(P^{*n*}Bu₃)₂ complex, and that the oxidative addition activation barriers are approximately 25 kcal/mol with Ni(P^{*n*}Bu₃)₂, while they are 3-5 kcal/mol higher with Ni(dcype). The remarkable difference in the coordination energy can be rationalized considering that the Ni(P^{*n*}Bu₃)₂ moiety has to deform from a P-Ni-P angle $\approx 180^\circ$ to $\approx 110^\circ$ upon coordination, see Figure 2b, whereas the geometry of the Ni(dcype) moiety, with a P-Ni-P angle $\approx 90^\circ$ enforced by the chelating ligand, see

Figure 2d, is nearly unchanged upon substrate coordination. Thus, we calculated the energy required to deform the metal fragment from the geometry it has before substrate coordination to the geometry it has after substrate coordination. According to these calculations deforming the relaxed Ni(PⁿBu₃)₂ moiety to the geometry it has upon coordination costs 10.9 kcal/mol more than deforming the Ni(dcype) moiety, almost accounting for the difference of 15.0 kcal/mol in the free energies of coordination. This conclusion is in line with similar considerations in the context of oxidative addition of aryl iodides to Au(I) complexes.³¹

Analysis of the transition state geometries, see Figure 2, allows understanding the origin of the different selectivity. In the C(acyl)-O activation transition states the substrate is oriented perpendicular to the P-Ni-P plane, with a η³ coordination of the substrate involving the activated C-O bond and the ipso C atom of the naphthyl moiety (Figures 2a and 2c). The forming Ni-C and Ni-O bonds and the Ni-P bonds assume an almost tetrahedral arrangement around the Ni atom, minimizing interaction between the substrate and the alkyl P-substituents. Differently, in the C(aryl)-C activation transition states the substrate is oriented in the P-Ni-P plane, with a η² coordination of the substrate involving only the activated C-C bond (Figures 2b and 2d). The forming Ni-C bonds and the Ni-P bonds assume an almost square planar arrangement around the Ni atom, maximizing interaction between the substrate and the alkyl P-substituents. This is particularly relevant with the Ni(PⁿBu₃)₂ system, due to the larger P-Ni-P angle, ≈110°, versus an angle ≈90° with the Ni(dcype) system. This is also evidenced by the steric maps reported (Figure S1),³² which indicate steric pressure by the PⁿBu₃ ligands in the coordination plane defined by the P-Ni-P bonds. The increased steric repulsion between the substrate and the PⁿBu₃ ligands destabilizes the C(aryl)-C activation transition state favoring C(acyl)-O activation.

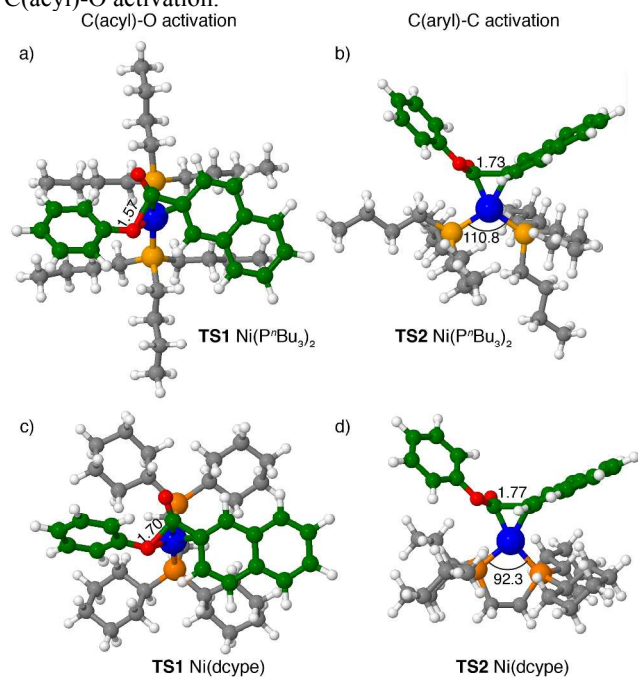


Figure 2. Parts a and b, geometry of transition states **TS1** and **TS2** for C(acyl)-O and C(aryl)-C activation with Ni(PⁿBu₃)₂. Parts c and d, geometry of transition states **TS1** and **TS2** for C(acyl)-O and C(aryl)-C activation with Ni(dcype). Distances

in Å and angles in deg. See Figure S1 for a different view of transition state TS2b.

Hammett Correlation Studies. In order to study the influence of the electronic effects of the substituents on the selective Suzuki-Miyaura coupling protocol, the magnitude of stabilization that occurred in the transition state for the coupling was determined from the Hammett analysis. Hammett plots were obtained by plotting $\log(k/k_0)$ against substituent parameter σ_p for the nickel catalyzed reaction of para-substituted phenolic ester derivatives with B-alkyl-9-BBN **2a**.³³ The plot of $\log(k/k_0)$ and σ_p for ketone formation gave a linear correlation with a slope $\rho = +1.2$ (Figure 3). The linear regression with σ_p value indicated that an inductive effect was mainly responsible for the stabilization of the transition state. The positive slope ($\rho = 1.2$) of the line indicated that oxidative addition of ester to Ni(0) was sensitive to the electronic effect of the substituents and weakening of the C(acyl)-O bond occurred. A positive nonzero slope for the Hammett indicates that oxidative-addition is the rate-determining step in ketone formation pathway. In contrast, for the decarbonylative process, the plot of $\log(k/k_0)$ against σ_p gave a linear correlation with a slope $\rho = -0.28$ (Figure 3). The linear regression with σ_p value indicated that oxidative addition is not the rate-determining step. Therefore, we considered investigating the full reaction mechanism by DFT calculations in the next stage. The possible DFT free energy profiles for the conversion of **10** to the final products are displayed in Figures 4a and 4b for Ni(PⁿBu₃)₂ and Ni(dcype), respectively.^{20c,30} Only the most favorable oxidative addition step (Figure 1) was considered for both catalysts. As discussed above, for Ni(PⁿBu₃)₂ the favored oxidative addition step leads to **IN1**. The following steps, from **IN1** to **IN9**, can be associated to the transmetalation section. It starts with PBu₃ dissociation, **IN1** to **IN4**, which costs only 10.6 kcal/mol in terms of Gibbs free energy, as the enthalpic penalty for PⁿBu₃ dissociation is compensated by a large increase in entropy. **IN4** can react with Cs₂CO₃ to remove CsOPh from the metal, leading to **IN5**. Coordination of ⁿPr-BBN to **IN5** leads to **IN6**, and the transmetalation step occurs via transition state **TS4** and an energy barrier of 21.2 kcal/mol from **IN5**.

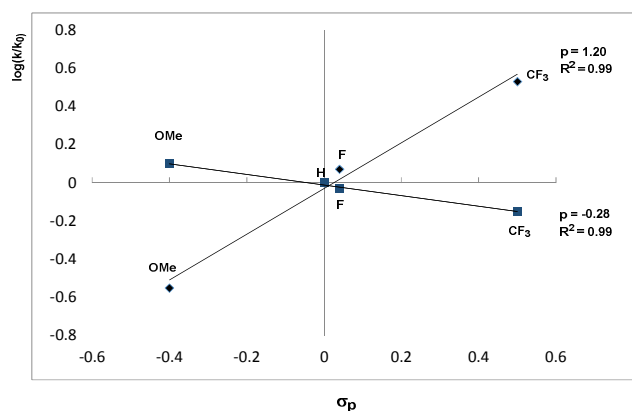
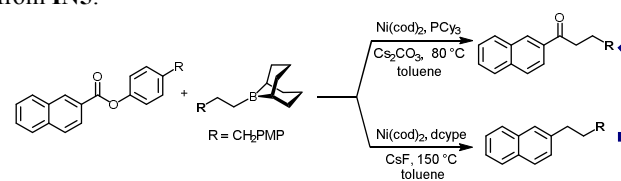
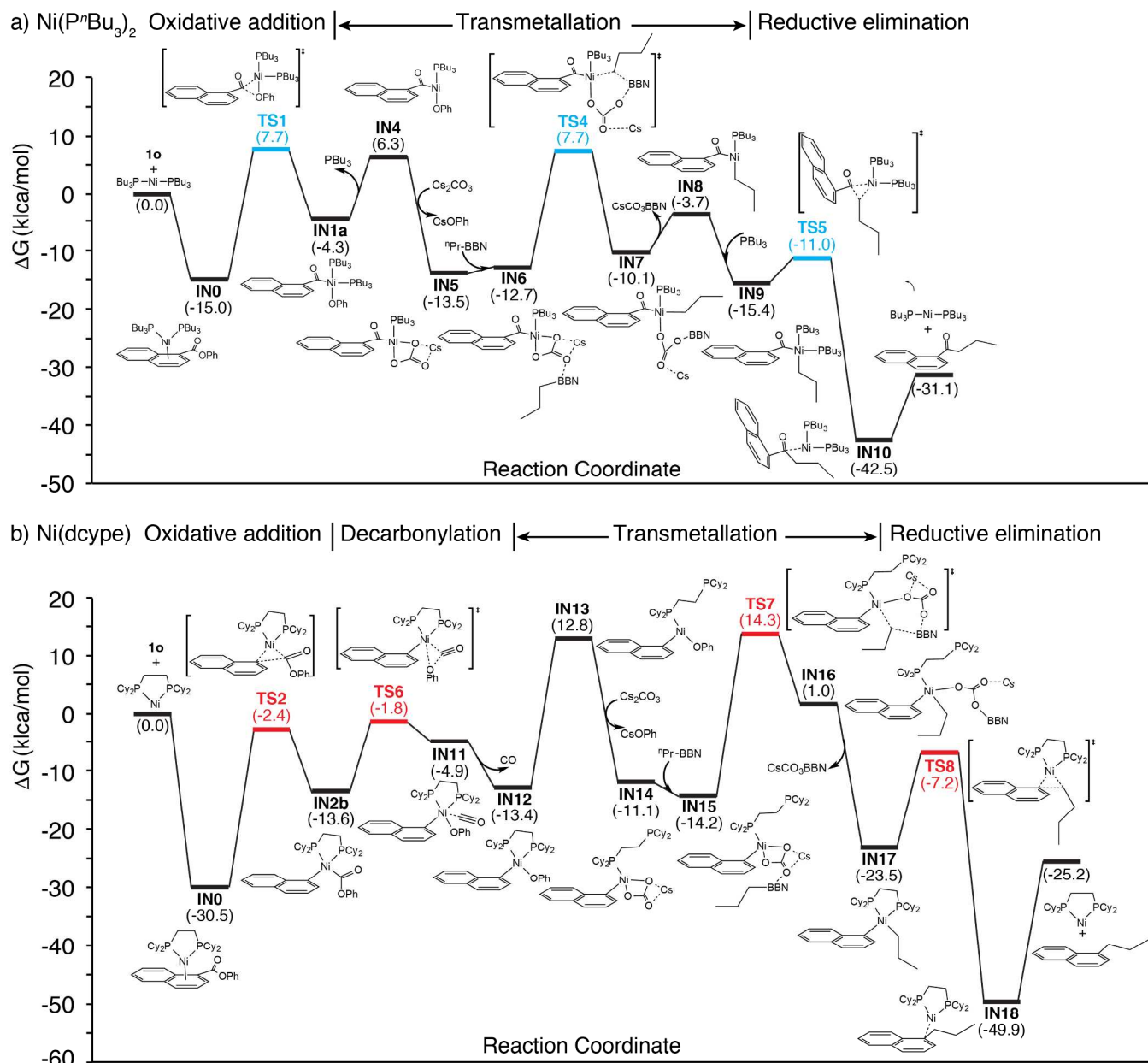


Figure 3. Hammett analysis of non-decarbonylative and decarbonylative Suzuki-Miyaura coupling using σ_p values.

Dissociation of $\text{Cs}(\text{CO}_3)\text{BBN}$ and coordination of a free P^nBu_3 ligand leads to **IN9** and completes the transmetallation section. The last step is reductive elimination from **IN9** via transition state **TS5** and an energy barrier of 4.4 kcal/mol only. Dissociation of the formed product from **IN10** requires 11.4 kcal/mol and regenerates the starting $\text{Ni}(\text{P}^n\text{Bu}_3)_2$ species. The reaction profile in Figure 4a indicates that, with $\text{Ni}(\text{P}^n\text{Bu}_3)_2$, the initial oxidative addition can be considered as the rate determining step, since it corresponds to the highest in energy transition state (**TS1** at 7.7 kcal/mol) and to the largest energy barrier (22.2 kcal/mol) from **IN0** to **TS1**. The transmetallation transition state **TS4** is at the same energy of **TS1**, but we can assume **TS4** as an upper bound limit, since more favorable pathways, eventually involving different aggregation states of the base, can be involved. To further support this scenario DFT Hammett plots were obtained by plotting $-\Delta\Delta E^\ddagger/\text{RT}$ against the substituent parameter σ_p of para-substituted phenolic ester derivatives of **1o** ($\Delta\Delta E^\ddagger$ is the difference in the energy of activation for oxidative addition of the C(acyl)-O bond to Ni between para-substituted and unsubstituted **1o**). The linear correlation between $-\Delta\Delta G^\ddagger/\text{RT}$ and σ_p with a positive slope (Figure S2) is in agreement with the experimental trend thus supporting the mechanistic rationalization. Moving to $\text{Ni}(\text{dcype})$, the favored oxidative addition step leads to **IN2**. Differently from the $\text{Ni}(\text{P}^n\text{Bu}_3)_2$ profile, calculations suggest that the next step is easy decarbonylation of **IN2** to **IN11**, via transition state **TS6** and an energy barrier of 11.8 kcal/mol, see Figure 4b. Exergonic CO dissociation leading to **IN12** completes the decarbonylation step. The transition state

for the competitive decarboxylation of **IN2** is calculated to be 11.1 kcal/mol above **TS6**, and thus this mechanistic option can be ruled out. The following steps, from **IN12** to **IN17**, correspond to the transmetallation section, with a mechanism strictly similar to that calculated for $\text{Ni}(\text{P}^n\text{Bu}_3)_2$, steps from **IN1** to **IN9**. Considering that reactivity with $\text{Ni}(\text{dcype})$ occurs with $\text{Cs}_2(\text{CO}_3)$ as well (see Table 5), for the sake of easier comparison with the $\text{Ni}(\text{P}^n\text{Bu}_3)_2$ energy profile we used $\text{Cs}_2(\text{CO}_3)$ instead of the better performing CsF. Details on the transmetallation step with CsF can be found in Figure S6. Transmetallation starts with dissociation of a P atom from Nickel, **IN12** to **IN13**, a step that costs 26.2 kcal/mol in terms of Gibbs free energy, as the tether between the two P atoms prevents a large increase in entropy that could compensate the enthalpic penalty. The high energy intermediate **IN13** can react with Cs_2CO_3 to remove CsOPh from the metal, leading to **IN14**. Coordination of $^n\text{Pr-BBN}$ to **IN14** leads to **IN15**, and the transmetallation step occurs via transition state **TS7** and an energy barrier of 28.5 kcal/mol from **IN15**. Dissociation of $\text{Cs}(\text{CO}_3)\text{BBN}$ from **IN16** and coordination of the dangling P atom leads to **IN17** completes the transmetallation section. The last step is reductive elimination from **IN17** via transition state **TS8** and an energy barrier of 16.3 kcal/mol. Dissociation of the formed product from **IN18** requires 24.7 kcal/mol and regenerates the starting $\text{Ni}(\text{P}^n\text{Bu}_3)_2$ species. The reaction profile in Figure 4b indicates that, with $\text{Ni}(\text{dcype})$, the highest in energy structure corresponds to the P dissociated intermediate **IN13**, an event triggering the transmetallation step. The transmetallation transition state **TS7** is at approximately the same energy of **IN13**. Again, we can assume **TS7** as an upper bound limit, since more favorable pathways eventually involving different aggregation states of the base can be involved.



39
40
41 **Figure 4.** Full DFT-computed Gibbs free energy (in kcal/mol) mechanism for the ligand-controlled nickel catalyzed Suzuki-Miyaura cross-coupling reactions with substrate **1o**, Cs_2CO_3 as the base, $^n\text{C}_3\text{H}_7\text{-BBN}$ as the organoboron reagent, for the a) $\text{Ni}(\text{P}^n\text{Bu}_3)_2$ and b) $\text{Ni}(\text{dcype})$ catalyts.

42
43
44
45 To further support this scenario DFT Hammett plots were
46 obtained by plotting $-\Delta\Delta E^{\text{Diss}}/\text{RT}$ against the substituent pa-
47 rameter σ_p of para-substituted phenolic ester derivatives of **1o**
48 ($\Delta\Delta E^{\text{Diss}}$ is the difference in the dissociation energy of the P
49 atom from **IN12** to give **IN13**, between para-substituted and
50 unsubstituted **1o**). The linear correlation between $-\Delta\Delta E^{\text{Diss}}/\text{RT}$
51 and σ_p with a negative slope (Figure S3) is in agreement with
52 the experimental trend. In contrast, DFT Hammett plots of $-\Delta\Delta E^{\ddagger}/\text{RT}$
53 for the oxidative addition of the C(aryl)-C(acyl)
54 bond to Ni via **TS2**, and for the decarbonylation step via **TS6**,
55 gave a linear correlation with a positive slope (see Figures S4
56 and S5), at odd with the experimental trend.

57 Considering decarbonylation of the oxidative addition in-

45
46
47
48
49
50
51
52
53
54
55
56
57
58
59
60
intermediate **IN2** irreversible, as the dissociated CO can escape
from solution, the mechanistic rationalization emerging from
Figures 3b and 4b suggests that the product selectivity deter-
mining step is the initial oxidative addition, while the rate
limiting step is connected to the transmetalation step.

CONCLUSIONS

In summary, the results reported herein represent the first
example of ligand-controlled and site-selective nickel cata-
lyzed Suzuki-Miyaura cross-coupling reaction with aromatic
ester and alkyl organoboron components as coupling partners.
This newly developed methodology enables a facile route for

C(sp²)-C(sp³) bond formation in a straightforward fashion by successful suppression of the undesired β-hydride elimination process. The switch in selectivity is attributed to the judicious choice of different phosphorus ligands, which notably converted the esters into the alkylated and ketone products respectively. The utility of this newly developed protocol has been demonstrated by the broad functional group tolerance and the application in the synthesis of bioactive compounds. DFT studies on the oxidative addition step of phenyl 2-naphthoate with different nickel complexes were carried out in order to rationalize this intriguing reaction chemoselectivity. When mono-dentate phosphorus ligands, such as PⁿBu₃ and PCy₃, were used, the nickel complex favors activation of the C(acyl)-O bond, which later generates the ketone product. On the other hand, the nickel complex with bi-dentate dcype ligand favors the C(aryl)-C bond cleavage in the oxidative addition step, leading to the alkylated product via a decarbonylative process. Complete DFT energy profiles indicate that, consistently with the experimental Hammett plots, the initial oxidative addition of the substrate is the rate limiting and product selectivity determining step when PⁿBu₃ is used as ligand. Differently, when dcype is used the initial oxidative addition of the substrate, followed by easy irreversible decarbonylation, is the product selectivity determining step, while transmetalation is rate limiting.

■ ASSOCIATED CONTENT

*Supporting Information

Experimental and computational details, full characterization of the products and spectra, Cartesian coordinates of the optimized geometries.

■ AUTHOR INFORMATION

Corresponding Author

* magnus.rueping@rwth-aachen.de *luigi.cavallo@kaust.edu.sa

Author Contributions

§A.C. and H.-H.L. contributed equally.

Notes

The authors declare no competing financial interest.

■ ACKNOWLEDGMENTS

H.-H.L. thanks the DAAD for a doctoral fellowship. A.P. thanks the Spanish MINECO for a project CTQ2014-59832-JIN. This research was supported by the KAUST Office of Sponsored Research under Award No. URF/1/3030-01. LC thanks the King Abdullah University of Science and Technology (KAUST) for supporting this work. For computer time, this research used the resources of the KAUST Supercomputing Laboratory (KSL) at KAUST.

■ REFERENCES

- (1) Suzuki, A. *Angew. Chem. Int. Ed.* **2011**, *50*, 6722-6737.
- (2) (a) Miyaura, N.; Suzuki, A. *Chem. Rev.* **1995**, *95*, 2457-2483. (b) Suzuki, A. *J. Organomet. Chem.* **1999**, *576*, 147-168. (c) Kotha, S.; Lahiri, K.; Kashinath, D. *Tetrahedron* **2002**, *58*, 9633-9695. (d) Maluenda, I.; Navarro, O. *Molecules* **2015**, *20*, 7528-7557.
- (3) For recent reviews on the C(sp²)-C(sp³) bond formation, see: (a) Chemler, S. R.; Trauner, D.; Danishefsky, S. J. *Angew. Chem. Int. Ed.* **2001**, *40*, 4544-4568. (b) Jana, R.; Pathak, T. P.; Sigman, M. S.

- Chem. Rev.* **2011**, *111*, 1417-1492. (c) Cherney, A. H.; Kadunce, N. T.; Reisman, S. E. *Chem. Rev.* **2015**, *115*, 9587-9652.
- (4) For pioneer works which utilized B-alkyl-9-BBNs as cross-coupling partners in nickel catalyzed carbon-halogen bond activation, see: (a) Saito, B.; Fu, G. C. *J. Am. Chem. Soc.* **2007**, *129*, 9602-9603. (b) Saito, B.; Fu, G. C. *J. Am. Chem. Soc.* **2008**, *130*, 6694-6695. (c) Owston, N. A.; Fu, G. C. *J. Am. Chem. Soc.* **2010**, *132*, 11908-11909. (d) Lu Z.; Fu, G. C. *Angew. Chem. Int. Ed.* **2010**, *49*, 6676-6678. (e) Lu Z.; Wilsily, A.; Fu, G. C. *J. Am. Chem. Soc.* **2011**, *133*, 8154-8157. (f) Zultanski, S. L.; Fu, G. C. *J. Am. Chem. Soc.* **2011**, *133*, 15362-15364. (g) Wilsily, A.; Tramutola, F.; Owston, N. A.; Fu, G. C. *J. Am. Chem. Soc.* **2012**, *134*, 5794-5797.
- (5) Brown, H. C.; Murray, K. J. *Tetrahedron* **1986**, *42*, 5497-5504.
- (6) (a) Blaser, H. U.; Spencer, A. J. *Organomet. Chem.* **1982**, *233*, 267-274; (b) Obora, Y.; Tsuji, Y.; Kawamura, T. *J. Am. Chem. Soc.* **1993**, *115*, 10414-10415. (c) Sugihara, T.; Satoh, T.; Miura, M.; Nomura, M. *Angew. Chem. Int. Ed.* **2003**, *42*, 4672-4674. (d) Sugihara, T.; Satoh, T.; Miura, M.; Nomura, M. *Adv. Synth. Catal.* **2004**, *346*, 1765-1772. (e) Sugihara, T.; Satoh, T.; Miura, M. *Tetrahedron Lett.* **2005**, *46*, 8269-8271. (f) Zhao, X.; Yu, Z. *J. Am. Chem. Soc.* **2008**, *130*, 8136-8137.
- (7) (a) Stephan, M. S.; Teunissen, A. J. J. M.; Verzijl, G. K. M.; Vries, J. G. de *Angew. Chem. Int. Ed.* **1998**, *37*, 662-664. (b) Brien, E. M. O.; Bercot, E. A.; Rovis, T. *J. Am. Chem. Soc.* **2003**, *125*, 10498-10499. (c) Yoshino, Y.; Kurahashi, T.; Matsubara, S. *J. Am. Chem. Soc.* **2009**, *131*, 7494-7495. (d) Jin, W.; Yu, Z.; He, W.; Ye, W.; Xiao, W.-J. *Org. Lett.* **2009**, *11*, 1317-1320.
- (8) (a) Meng, G.; Szostak, M.; *Angew. Chem. Int. Ed.* **2015**, *54*, 14518-14522. For reviews on the application of amides in cross coupling reactions, see: (b) Meng, G.; Shi, S.; Szostak, M. *Synlett* **2016**, *27*, 2530-2540. (c) Dander, J. E.; Garg, N. K. *ACS Catal.* **2017**, *7*, 1413-1423. (d) Liu, C.; Szostak, M. *Chem. Eur. J.* **2017**, *23*, 7157-7173.
- (9) (a) Gooßen, L. J.; Paetzold, J. *Angew. Chem. Int. Ed.* **2002**, *41*, 1237-1241. (b) Gooßen, L. J.; Paetzold, J. *Angew. Chem. Int. Ed.* **2004**, *43*, 1095-1098. (c) Gribkov, D. V.; Pastine, S. J.; Schnürch, M.; Sames, D. *J. Am. Chem. Soc.* **2007**, *129*, 11750-11755. (d) Okita, T.; Kumazawa, K.; Takise, R.; Muto, K.; Itami, K.; Yamaguchi, J. *J. Chem. Lett.* **2017**, *46*, 218-220. For Ni-catalyzed decarbonylative cross coupling reactions with esters, see: (e) Amaike, K.; Muto, K.; Yamaguchi, J.; Itami, K. *J. Am. Chem. Soc.* **2012**, *134*, 13573-13576. (f) Meng, L.; Kamada, Y.; Muto, K.; Yamaguchi, J.; Itami, K. *Angew. Chem., Int. Ed.* **2013**, *52*, 10048-10051. (g) Correa, A.; Cornella, J.; Martin, R. *Angew. Chem. Int. Ed.* **2013**, *52*, 1878-1880. (h) Muto, K.; Yamaguchi, J.; Musaev, D. G.; Itami, K. *Nat. Commun.* **2015**, *6*, 7508. (i) LaBerge, N. A.; Love, J. A. *Eur. J. Org. Chem.* **2015**, 5546-5553. (j) Desnoyer, A. N.; Friese, F. W.; Chiu, W.; Drover, M. W.; Patrick, B. O.; Love, J. A. *Chem. Eur. J.* **2016**, *22*, 4070-4077. (k) Guo, L.; Chatupheeraphat, A.; Rueping, M. *Angew. Chem., Int. Ed.* **2016**, *55*, 11810-11813. (l) Guo, L.; Rueping, M. *Chem. Eur. J.* **2016**, *22*, 16787-16790. (m) Pu, X.; Hu, J.; Zhao, Y.; Shi, Z. *ACS Catal.* **2016**, *6*, 6692-6698. (n) Amaike, K.; Itami, K.; Yamaguchi, J. *Chem.-Eur. J.* **2016**, *22*, 4384-4388. (o) Takise, R.; Isshiki, R.; Muto, K.; Itami, K.; Yamaguchi, J. *J. Am. Chem. Soc.* **2017**, *139*, 3340-3343. (p) Yue, H.; Guo, L.; Liao, H. H.; Cai, Y.; Zhu, C.; Rueping, M. *Angew. Chem. Int. Ed.* **2017**, *56*, 4282-4285. (q) Yue, H.; Guo, L.; Lee, S. C.; Liu, X.; Rueping, M. *Angew. Chem. Int. Ed.* **2017**, *56*, 3972-3976. (r) Liu, X.; Jia, J.; Rueping, M. *ACS Catal.* **2017**, *7*, 4491-4496. (s) Chatupheeraphat, A.; Liao, H.-H.; Lee, S.-C.; Rueping, M. *Org. Lett.* **2017**, *19*, 4255-4258. For a recent review, see: (t) Takise, R.; Muto, K.; Yamaguchi, J. *Chem. Soc. Rev.* **2017**, *46*, 5864-5888.
- (10) (a) Rosen, B. M.; Quasdorf, K. W.; Wilson, D. A.; Zhang, N.; Resmerita, A.-M.; Garg, N. K.; Percec, V. *Chem. Rev.* **2011**, *111*, 1346-1416. (b) Tasker, S. Z.; Standley, E. A.; Jamison, T. F. *Nature* **2014**, *509*, 299-309. (c) Ananikov, V. P. *ACS Catal.* **2015**, *5*, 1964-1971.
- (11) (a) Koga, N.; Obara, Shigeru.; Kitaura, K.; Morokuma, K. *J. Am. Chem. Soc.* **1985**, *107*, 7109-7116. (b) Lin, B.-L.; Liu, L.; Fu, Y.; Luo, S.-W.; Chen, Q.; Guo, Q.-X. *Organometallics* **2004**, *23*, 2114-2123.
- (12) For the nickel catalyzed inert bond activation with β-hydrogen containing organometallic reagents, see: with alkylaluminum reagents,

gents: (a) Liu, X.; Hsiao, C.-C.; Kalvet, I.; Leiendecker, M.; Guo, L.; Schoenebeck, F.; Rueping, M. *Angew. Chem., Int. Ed.* **2016**, *55*, 6093-6098. with alkylmagnesium reagents: (b) Tobisu, M.; Takahira, T.; Morioka, T.; Chatani, N. *J. Am. Chem. Soc.* **2016**, *138*, 6711-6714; with alkylborane reagents: (c) Guo, L.; Hsiao, C.-C.; Yue, H.; Liu, X.; Rueping, M. *ACS Catal.* **2016**, *6*, 4438-4442. (d) Guo, L.; Liu, X.; Baumann, C.; Rueping, M. *Angew. Chem. Int. Ed.* **2016**, *55*, 15415-15419; with alkylzinc reagents: (e) Simmons, B. J.; Weires, N. A.; Dander, J. E.; Garg, N. K. *ACS Catal.* **2016**, *6*, 3176-3179.

(13) Jorgenson, M. J. *Org. React.* **1970**, *18*, 1-97.

(14) (a) Blangetti, M.; Rosso, H.; Prandi, C.; Deagostino, A.; Venturello, P. *Molecules* **2013**, *18*, 1188-1213. (b) Meng, G.; Szostak, M. *Org. Biomol. Chem.* **2016**, *14*, 5690-5707. (c) Mondal, M.; Begum, T.; Bora, U. *Org. Chem. Front.* **2017**, *4*, 1430-1434.

(15) (a) Haddach, M.; McCarthy, J. R. *Tetrahedron Lett.* **1999**, *40*, 3109-3112. (b) Raffee F.; Hajipour, A. R. *Appl. Organomet. Chem.* **2015**, *29*, 181-184. (c) Semler, M.; Štěpnička, P. *Catal. Today* **2015**, *243*, 128-133. (d) Forbes, A. M.; Meier, G. P.; Jones-Mensah, E.; Magolan, J. *Eur. J. Org. Chem.* **2016**, 2983-2987.

(16) Chen, Q.; Fan, X.-H.; Zhang, L.-P.; Yang, L.-M. *RSC Adv.* **2014**, *4*, 53885-53890.

(17) (a) Liebeskind, L. S.; Srogi, J. *J. Am. Chem. Soc.* **2000**, *122*, 11260-11261. (b) Yu, Y.; Liebeskind, L. *J. Org. Chem.*, **2004**, *69*, 3554-3557. (c) Savarin, C.; Srogi, J.; Liebeskind, L. S. *Org. Lett.*, **2000**, *2*, 3229-3231. (d) Zeysing, B.; Gosch, C.; Terfort, A. *Org. Lett.*, **2000**, *2*, 1843-1845. (e) Prokopcová, H.; Kappe, C. O. *Angew. Chem., Int. Ed.* **2009**, *48*, 2276-2286.

(18) (a) Li, X.; Zou, G. *J. Organomet. Chem.* **2015**, *794*, 136-145. (b) Meng, G.; Szostak, M. *Org. Lett.* **2015**, *17*, 4364-4367. (c) Li, X.; Zou, Z. *Chem. Commun.* **2015**, *51*, 5089-5092. (d) Weires, N. A.; Baker, E. L.; Garg, N. K. *Nat. Chem.* **2016**, *8*, 75-79. (e) Meng, G.; Shi, S.; Szostak, M. *ACS Catal.* **2016**, *6*, 7335-7339. (f) Shi, S.; Szostak, M. *Org. Lett.* **2016**, *18*, 5872-5875. (g) Liu, C.; Meng, G.; Liu, Y.; Liu, R.; Lalancette, R.; Szostak, R.; Szostak, M. *Org. Lett.* **2016**, *18*, 4194-4197. (h) Lei, P.; Meng, G.; Szostak, M. *ACS Catal.* **2017**, *7*, 1960-1965. (i) Liu, C.; Liu, Y.; Liu, R.; Lalancette, R.; Szostak, R.; Szostak, M. *Org. Lett.* **2017**, *19*, 1434-1437. (j) Ni, S.; Zhang, W.; Mei, H.; Han, J.; Pan, Y. *Org. Lett.* **2017**, *19*, 2536-2539. (k) Amani, J.; Alam, R.; Badir, S.; Molander, G. A. *Org. Lett.* **2017**, *19*, 2426-2429. (l) Shi, S.; Szostak, M. *Synthesis* **2017**, *49*, 3602-3608. (m) Lei, P.; Meng, G.; Ling, Y.; An, J.; Szostak, M. *J. Org. Chem.* **2017**, *82*, 6638-6646. (n) Meng, G.; Szostak, R.; Szostak, M. *Org. Lett.* **2017**, *19*, 3596-3599. (o) Meng, G.; Lalancette, R.; Szostak, R.; Szostak, M. *Org. Lett.* **2017**, *19*, 4656-4659.

(19) Yamamoto, T.; Ishizu, J.; Kohara, T.; Komiyama, S.; Yamamoto, A. *J. Am. Chem. Soc.* **1980**, *102*, 3758-3764.

(20) (a) Tatamidani, H.; Yokota, K.; Kakiuchi, F.; Chatani, N. *J. Org. Chem.* **2004**, *69*, 5615-5621. (b) Tatamidani, H.; Kakiuchi, F.; Chatani, N. *Org. Lett.* **2004**, *6*, 3597-3599. For more recent Pd-catalyzed protocols, see: (c) Halima, T. B.; Zhang, W.; Yalaoui, I.; Hong, X.; Yang, Y.-F.; Houk, K. N.; Newman, S. G. *J. Am. Chem. Soc.* **2017**, *139*, 1311-1318. (d) Lei, P.; Meng, G.; Shi, S.; Ling, Y.; An, J.; Szostak, R.; Szostak, M. *Chem. Sci.* **2017**, *8*, 6525-6530. (e) Isshiki, R.; Takise, R.; Itami, K.; Muto, K.; Yamaguchi, J. *Synlett* **2017**, *28*, 2599-2603.

(21) A mixture of decarbonylative and ketone product was obtained in previous studies without full control of the alkylated or ketone products, see: Gooßen, L. J.; Paetzold. *Adv. Synth. Catal.* **2004**, *346*, 1665-1668. See also ref 9i.

(22) Bond enthalpy data were taken from (accessed on 27/09/2016), http://www.wiredchemist.com/chemistry/data/bond_energies_lengths.html.

(23) Nilsson, P.; Olofsson, K.; Larhed, M. Microwave-Assisted and Metal-Catalyzed Coupling Reactions in *Topics in Current Chemistry. Microwave Methods in Organic Synthesis*; Larhed, M.; Olofsson, K. Eds.; Springer: Heidelberg, 2006; Vol. 266, pp 103-144.

(24) (a) Shi, S.; Meng, G.; Szostak, M. *Angew. Chem. Int. Ed.* **2016**, *55*, 6959-6963. (b) Hu, J.; Zhao, Y.; Liu, J.; Zhang, Y.; Shi, Z. *Angew. Chem. Int. Ed.* **2016**, *55*, 8718-8722. For further Ni-catalyzed decarbonylative transformations of amides, see: (c) Dey, A.; Sasmal, S.; Seth, K.; Lahiri, G. K.; Maiti, D. *ACS Catal.* **2017**, *7*, 433-437. (d) Srimontree, W.; Chatupheeraphat, A.; Liao, H.-H.; Rueping, M. *Org. Lett.* **2017**, *19*, 3091-3094. (e) Liu, X.; Yue, H.; Jia, J.; Guo, L.; Rueping, M. *Chem. Eur. J.* **2017**, *23*, 11771-11775. (f) Liu, C.; Szostak, M. *Angew. Chem. Int. Ed.* **2017**, *56*, 12718-12722. (g) Hu, J.; Wang, M.; Pu, X.; Shi, Z. *Nat. Commun.* **2017**, *8*, 14993. (h) Lee, S.-C.; Guo, L.; Yue, H.; Liao, H.-H.; Rueping, M. *Synlett* **2017**, *28*, 2594-2598.

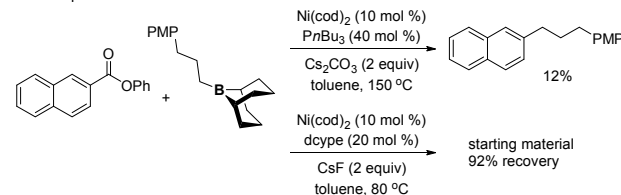
(25) See the Supporting Information for details.

(26) De Corte, B. L.; Kinney, W. A.; Liu, Li.; Ghosh, S.; Brunner, L.; Hoekstra, W. J.; Santulli, R. J.; Tuman, R. W.; Baker, J.; Burns, C.; Proost, J. C.; Tounge, B. A.; Damiano, B. P.; Maryanoff, B. E.; Johnson, D. L.; Gallema R. A. Jr. *Bioorg. Med. Chem. Lett.* **2004**, *14*, 5227-5232.

(27) Orjales, A.; Mosquera, R.; Toledo, A.; Pumar, M. C.; García N.; Cortizo L.; Labeaga, L.; Innerarity A. *J. Med. Chem.* **2003**, *46*, 5512-5532.

(28) To rule out the intermediary ketone formation in the decarbonylative alkylation process, ketone **7a** was subjected to the reaction conditions of Table 2. However, no ketone decarbonylation was observed. In addition, a control experiment was carried out to understand the correlation between ligand and temperature. When we used the Ni/P^tBu₃ complex at high temperature (150 °C), the decarbonylative product was obtained in 12% yield. On the other hand, when we used the Ni/dcype complex at lower temperature (80 °C), no ketone product was observed.

Cross-experiment



(29) Free energies in toluene were estimated using the M06 functional as implemented in Gaussian09, with the all electron def2-tzvp basis set. Electrostatic and non-electrostatic solvent effects were estimated with the SMD solvation model.

(30) For related theoretical studies, see: (a) Yoshikai, N.; Matsuda, H.; Nakamura, E. *J. Am. Chem. Soc.* **2008**, *130*, 15258-15259. (b) Li, Z.; Zhang, S. L.; Fu, Y.; Guo, Q. X.; Liu, L. *J. Am. Chem. Soc.* **2009**, *131*, 8815-8823. (c) Hong, X.; Liang, Y.; Houk, K. N. *J. Am. Chem. Soc.* **2014**, *136*, 2017-2025. (d) Lu, Q.; Yu, H.; Fu, Y. *J. Am. Chem. Soc.* **2014**, *136*, 8252-8260. (e) Xu, H.; Muto, K.; Yamaguchi, J.; Zhao, C.; Itami, K.; Musaev, D. G. *J. Am. Chem. Soc.* **2014**, *136*, 14834-14844. For reviews on mechanistic studies on Ni-catalyzed cross-coupling reactions, see: (f) Li, Z.; Liu, L. *Chin. J. Catal.* **2015**, *36*, 3-14. (g) Sperger, T.; Sanhueza, I. A.; Kalvet, I.; Schoenebeck, F. *Chem. Rev.* **2015**, *115*, 9532-9586.

(31) (a) Joost, M.; Zeineddine, A.; Estévez, L.; Mallet-Ladeira, S.; Miqueu, K.; Amgoune, A.; Bourissou, D. *J. Am. Chem. Soc.* **2014**, *136*, 14654-14657. (b) Fernández, I.; Wolters, L. P.; Bickelhaupt, F. M. *J. Comput. Chem.* **2014**, *35*, 2140-2145.

(32) Falivene, L.; Credendino, R.; Poater, A.; Petta, A.; Serra, L.; Oliva, R.; Scarano, V.; Cavallo, L. *Organometallics* **2016**, *35*, 2286-2293.

(33) Hansch, C.; Leo, A.; Taft, R. W. *Chem. Rev.* **1991**, *91*, 165-195.

Graphic Material for the Table of Contents

